Pergamon

Prog. Quant. Electr. 1997, Vol. 21, No. 2 pp. 81–108

Printed in Great Britain

PII: S0079-6727(96)00002-X

0079-6727/97 $32.00

SUPERLUMINAL PHOTONIC TUNNELING AND QUANTUM ELECTRONICS

GÜNTER NIMTZ and WINFRIED HEITMANN

II. Physikalisches Institut, Universität zu Köln, D-50937, Köln, Germany

Abstract—Recent experimental studies with microwave and laser pulses have revealed superluminal (faster-than-light) group, signal and energy velocities for the tunneling of electromagnetic wave packets in undersized waveguides and other photonic barriers. First we report on the historic background of tunneling and the problems of the interpretation of electronic tunneling data. The mathematical analogy of the classical tunneling, i.e. the propagation of evanescent modes, described by the Helmholtz equation, and the quantum mechanical tunneling, described by the Schrödinger equation, is introduced. In the next sections the experimental data on the tunneling time of electromagnetic wave packets and signals is presented. The interpretation of the experimental observations, particularly the production of superluminal tunneling velocity and its implication for the quantum mechanical electronic tunneling are discussed in the following sections. An introduction to the various theoretical approaches is included. Remarks on superluminal tunneling and on causality conclude the paper. Copyright © 1997 Elsevier Science Ltd

Contents

1. INTRODUCTION

Electronic tunneling in solid state physics has been evidenced in the 1950s and has been extensively investigated since that time. Especially tunneling junctions have been studied, where an electrical insulator forming a potential barrier is sandwiched between a superconductor and a normal conductor.[1] Other important examples for tunneling in solid state physics represent the semiconductor tunneling diode[2] and the tunneling microscope.[3] However, one important question has not been settled all the time: the duration of the tunneling process. The time spent by a wave packet traversing the barrier has been a subject of discussions for more than half a century.[4-6] In the case of electronic tunneling, it has not been possible to measure this time unambiguously.[7,8] The problems are the extremely short times and even if a time has been measured, it may have been determined by processes other than the tunneling process, as e.g. by the Coulomb interaction of the electrons with its charged environment.

Recently, the discussion of the tunneling time problem has experienced a new stimulus by the results of analogous experiments with evanescent electromagnetic wave packets. Spectacularly they have revealed even superluminal tunneling velocities, i.e. the measured barrier traversal time for electromagnetic wave packets and for AM-signals correspond to velocities faster than light. The first superluminal results were obtained with microwave signals by Enders and Nimtz.[9,10] The superluminal microwave tunneling data (the velocities in question are defined in Section 3.1) were confirmed in an averaged single photon experiment by Steinberg *et al.*,[11] in a further microwave experiment by Ranfagni *et al.* with leaky waves,[12] and with laser pulses by Spielmann *et al.*[13] All the experimental results have shown, that earlier quantum mechanical phasetime calculations (Hartman[14]) do describe the barrier traversal time, and thus for example enable one to determine the dynamical specification of a micro-electronic tunneling device.

In this article we shall introduce the electromagnetic tunneling analogy and present some experimental results, and we shall discuss the essentials of the theoretical investigations on the tunneling time problem. Finally we shall briefly mention the causality problem, which has received much attention in the physicists' community and in the media quite recently, see e.g.[15]

A conclusion of all the photonic investigations is that the quantum mechanical approaches do describe the dynamical behaviour of the tunneling process.

1.1. *Historical remarks*

One century ago Bose carried out classical tunneling experiments, i.e. the decay of evanescent waves.[16,17] He measured the intensity of cm-wave signals transmitted through two prisms which depended on the distance between them. The rather large prisms were made from tar.[17] The chosen incident angle of the cm-waves beam was larger than that of total reflection. At distances shorter than the wavelength he found a finite transmission into the second prism across the air gap. This quasi-optical experiment corresponds to the non-classical tunneling process as shown in Fig. 1(b). Bose found a strong dependence of the transmission of the cm-waves on the gap length between the two prisms. Much later also optical evanescent modes were theoretically and experimentally investigated, see e.g.[18] However, the propagation time and velocity of the evanescent modes have not been measured until recently.

1.2. *The analogy: Helmholtz's and Schrödinger's equations*

The Helmholtz equation follows from Maxwell's equations in a charge-free space

$$\nabla \cdot E = 0;\ \nabla \times E + \frac{1}{c}\frac{\partial B}{\partial t} = 0$$

$$\nabla \cdot B = 0;\ \nabla \times B - \frac{\mu\epsilon}{c}\frac{\partial E}{\partial t} = 0.$$

For every Cartesian component of the electromagnetic fields we obtain the wave equation.

$$\Delta E - \frac{\mu\epsilon}{c^2}\frac{\partial^2 E}{\partial t^2} = 0$$

where μ and ϵ are the free-space magnetic and electric permeabilities and c the velocity of light in vacuum.

The solution in one dimension is represented by a plane wave, for example for the electric field component

$$E_k(x,t) = E_0 \exp(ikx - i\omega t)$$

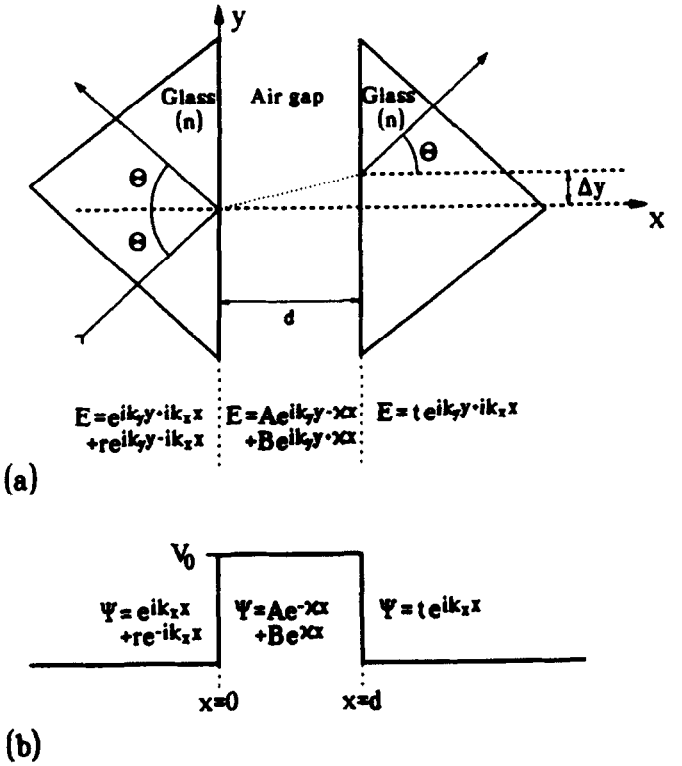

Fig. 1. The classical optical tunnel analogy: (a) total reflection at a double-prism and its corresponding quantum mechanical wave barrier. Total reflection takes place at the transition from high to low refractive index matter. (b) The gap between the prisms corresponds to the quantum mechanical barrier length.

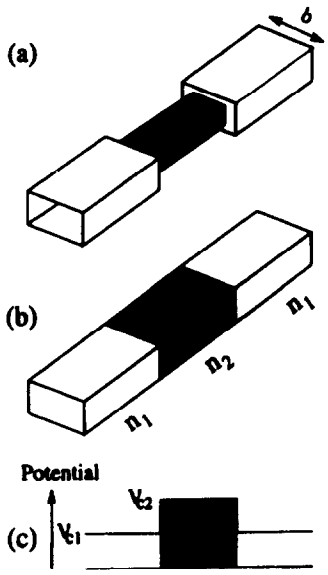

Fig. 2. (a) Rectangular waveguide with a part of reduced cross section in the center. (b) Rectangular wave guide filled with dielectric media with refractive indexes n_1 and n_2 with $n_1 > n_2$. (c) Sketch of the corresponding photonic potential.

where x and t are the Cartesian space component and the time, respectively, and k and ω are the wave number and the angular frequency, respectively. This solution put into the wave equation yields the Helmholtz equation for the electric field component in waveguides

$$\frac{\partial^2}{\partial z^2} E + \frac{\mu\epsilon}{c^2}\left(\omega^2 - \omega_c^2\right)E = 0$$

This equation for the propagation of a scalar field is formally identical to the Schrödinger equation for the wave function ψ.

$$\frac{\partial^2}{\partial z^2}\psi + \frac{2m}{\hbar^2}(W - U)\psi = 0$$

where m is the particle's mass, $\hbar$ the Planck constant, W the energy, and U a uniform potential energy.

We can write an analogous relation for the refractive index

$$n\frac{\omega}{c} = \sqrt{\mu\epsilon}\,\frac{\omega}{c} \equiv \sqrt{\frac{2m}{\hbar^2}(W - U)}$$

which means that, a quantum mechanical particle with the energy W in the potential energy U corresponds to an electromagnetic wave of frequency ω in a medium characterized by the refractive index n.

The direct mathematical analogy between one-dimensional quantum tunneling of particles and evanescent electromagnetic waves in a waveguide has been studied by Martin and Landauer.[19] They have demonstrated that the boundary conditions at the interface between a propagating and an evanescent region of a waveguide (see Section 2.1) with the same cross section but different refractive index lead to the same transmission and reflection coefficients as for a square-barrier tunneling problem. An example of such a waveguide with constant

cross section but with an abrupt change in refractive index is sketched in Fig. 2(b). It has been shown by Brodowsky *et al.*,[20] that the waveguide structure with a reduced cross section yields the same tunneling results as the waveguide filled with a dielectric material of reduced refractive index.

2. PHOTONIC BARRIERS

Based on this formal analogy, tunneling time experiments were started using undersized microwave waveguides by Ranfagni *et al.* in 1991.[21,12] Similar microwave experiments were carried out by Enders and Nimtz in both time- and frequency-domain in 1992.[9] The provoking result of the latter study has been a very short barrier traversal time, which corresponds to superluminal (faster-than-light) tunneling velocity. Experiments carried out with optical techniques confirmed the superluminal barrier crossing somewhat later than the microwave experiments. In the optical experiments barriers of periodic dielectric heterostructures, i.e. of dielectric mirrors, were used. They have forbidden bandgaps like electronic band gaps in a semiconductor. The gaps are often called stopbands. The imaginary wave number solutions of the forbidden bands have dispersion relations different from those of undersized waveguides or of the quantum mechanical square potential. Again, the experiments with such mirrors have revealed superluminal barrier crossing for single photons,[11] for laser pulses,[13] and for microwave packets.[22] In the following sections the two types of electromagnetic wave barriers are introduced.

2.1. *Undersized waveguides*

In general, for wave propagation to be possible, a guide's cross section has to exceed half the wavelength. In the case of a rectangular waveguide this condition has to be fulfilled for the basic mode (TE_{01}) only in one of the transverse directions, see e.g.[23] We shall demonstrate this condition for a wave guide formed by a rectangular metal tube. These guides have been used in the tunneling time microwave experiments. Two different undersized rectangular guides are shown in Fig. 2. Part (a) of the figure shows a hollow guide with a narrow portion in the center, corresponding to a higher cut-off frequency, whereas in part (b) the guide has a uniform cross section but is filled with two dielectric materials of different refractive index n. If the condition $n_1 > n_2$ holds, the photonic potential has a structure as displayed in part (c) of this illustration. For the basic propagating TE_{10}-mode in a rectangular waveguide the dispersion is given by

$$k_i^2 = \left(\frac{2\pi\nu n_i}{c}\right)^2\left(1 - \left(\frac{\nu_{ci}}{\nu}\right)^2\right)$$

where ν is the wave's frequency, $\nu_{ci} = c/2bn_i$ is the cut-off frequency of the guide with the width b (b being the broad side of the rectangular waveguide). $\lambda_{ci} = c/\nu_{ci}$ is the cut-off wavelength of the guide.

In case the frequency becomes lower than the cut-off frequency the wave number is purely imaginary. The propagation is stopped, and the field intensity decays exponentially with distance in the undersized part of the wave guide. Thus we have the analogous behaviour as in the case of a square potential barrier. Waves having frequencies $\nu < \nu_{ci}$ are tunneling modes or evanescent modes. The boundary condition for E in the case of the waveguide configuration (b) of Fig. 2 has been shown to be identical with those of the wave function ψ in the case of a one-dimensional barrier.[19] The geometrical discontinuities of the structure of case (a) has no significant influence on the transmission coefficient.[20]

2.2. *Periodic dielectric heterostructures*

Periodic heterostructures, independently of being of an electronic, photonic or acoustic nature, have frequency regimes of wave propagation and regimes of forbidden propagation. The general wave propagation in periodic structures has been presented by Brillouin.[24] In the case of forbidden propagation the wave number becomes imaginary similar to the evanescent modes in an undersized wave guide. The basic principle for this behaviour, either of being transparent or being total reflecting, is the interference of the multiple reflected wave. Such periodic heterostructures are used in many optical and electrotechnical devices, as filters or to improve the transmission. With respect to the tunneling discussed here, only one-dimensional structures have been used. However, recently many studies have been devoted to three-dimensional photonic lattice structures.[25] They have interesting optoelectronic device aspects, for example in improving light emitting diodes by inhibiting the spontaneous emission. This can be achieved, if the device's environment has a photonic crystal structure with a forbidden band gap at the frequencies to be inhibited.

Figure 3 shows a one-dimensional periodic dielectric hetero-structure. Such structures have forbidden band gaps (stopbands), which represent frequency regions where the solutions for the fields are corresponding to those of the evanescent modes (tunneling modes) in undersized wave guides. Of course band gaps have a quite different dispersion relation compared with that of an undersized waveguide as sketched in Fig. 3(c). The barrier transmission time for such structures has been studied with single photons,[11] with microwaves,[22] and with laser pulses.[13] There have been observed superluminal traversal velocities in the forbidden frequency region also.

We shall give in the following some details of a one-dimensional photonic lattice similar to that used in the microwave and in the optical experiments.[26] Review articles on three-dimensional photonic lattice structures have been written for example by Yablonovitch[25] and Villeneuve and Piché.[27]

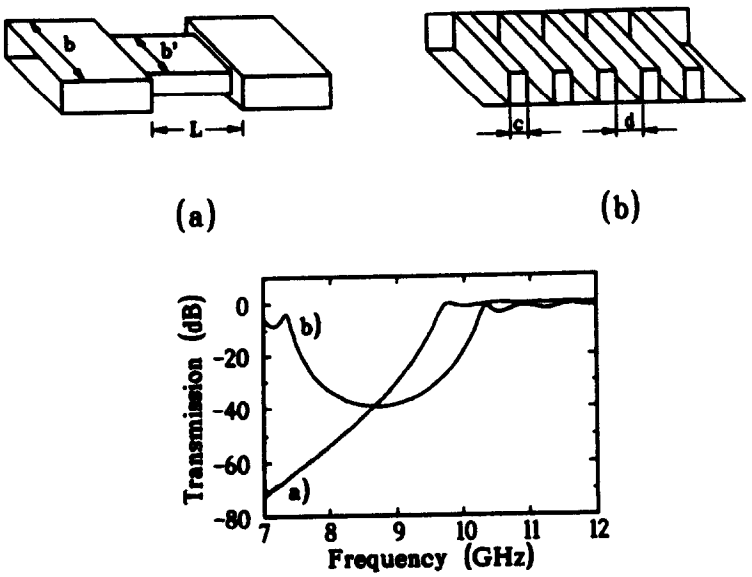

Fig. 3. Examples (a) of a waveguide with an undersized central part and (b) a one-dimensional periodic dielectric hetero-structure. In (c) the graphs show the dispersion relations for both structures. The transmission dispersion of the periodic heterostructure displays a forbidden gap which corresponds to a tunneling regime.

In the case presented here, the periodic dielectric heterostructure is constructed from 3 or 7 layers of Plexiglas (6 mm thick, refractive index $n = 1.6$) separated by air layers (9.6 mm thick). The transmission t, the reflection r, and the phase shift ϕ were calculated for electric field amplitudes. E_{j-1} and E_j are the electric fields in the media at the left and right hand side of the jth boundary. Continuity of the fields at the boundaries are assumed in the calculations. With x_j the position of the boundaries in the x-direction the complex transmission properties of the structure are calculated with the relations

$$E_{j-1}(x_j) = E_j(x_j)$$

$$E'_{j-1}(x_j) = E_j'(x_j)$$

$$E_j(x) = a_j e^{ik_j x} + b_j e^{ik_j x}$$

$$k_j = \frac{\omega}{c}\left(\epsilon_j\right)^{1/2}$$

$$t = \frac{a_m e^{ik_m x_m}}{a_0 e^{ik_0 x_1}}$$

$$r = \frac{b_0 e^{-ik_0 x_1}}{a_0 e^{ik_0 x_1}}$$

$$|t^2| + |r^2| = 1$$

$$j \in [1,m].$$

The data are presented in Fig. 4. The graphs show the dependence of the stopband on frequency for three and seven Plexiglas layers. In part (b) with a larger frequency range a second forbidden band is seen. The phase shift of the transmitted wave is shown in part (c), in the forbidden frequency regime the phase shift becomes very small. The group velocity calculated from the phase time (definition in Section 4.1) is shown in part (d). In the forbidden frequency regime the group velocity may be also superluminal as observed in optical and microwave experiments.[11, 13, 22]

3. PHOTONIC TUNNELING TIME EXPERIMENTS

3.1. *Electromagnetic wave packets and AM signals*

The first superluminal tunneling experiments were carried out with microwave packets and with AM-signals.[9] Results are shown in Figs 5 and 6. The experiments were carried out with pulses (frequency band limited and Gaussian-like) in the frequency domain technique as well as with AM-signals in the time domain technique.[9] (The frequency domain technique is a modern and very useful measuring method to determine the complex transmission function with a precision not achieved before. Within a well defined frequency window and an extremely high resolution, the amplitude and the phase shift are measured as functions of frequency. The experimental transmission data are then transformed into the time domain by Fourier transforms.) Both experiments with the pulses as well as with the AM-signals revealed group velocities $> c$ in traversing an undersized waveguide or a periodic dielectric heterostructure in the forbidden frequency regime.[9, 10, 22]

Recently Aichmann and Nimtz have demonstrated in a simple time domain experiment, that frequency band limited signals can exceed the velocity of light.[28] The experimental set-up is sketched in Fig. 7. Mirror M_1 has a splitting ratio of 1:40 in order to compensate the strong reflection loss due to the tunnel barrier (it will be shown later that the magnitude of a signal does not influence its velocity). Barrier length and air distance are calibrated having 11.42 cm

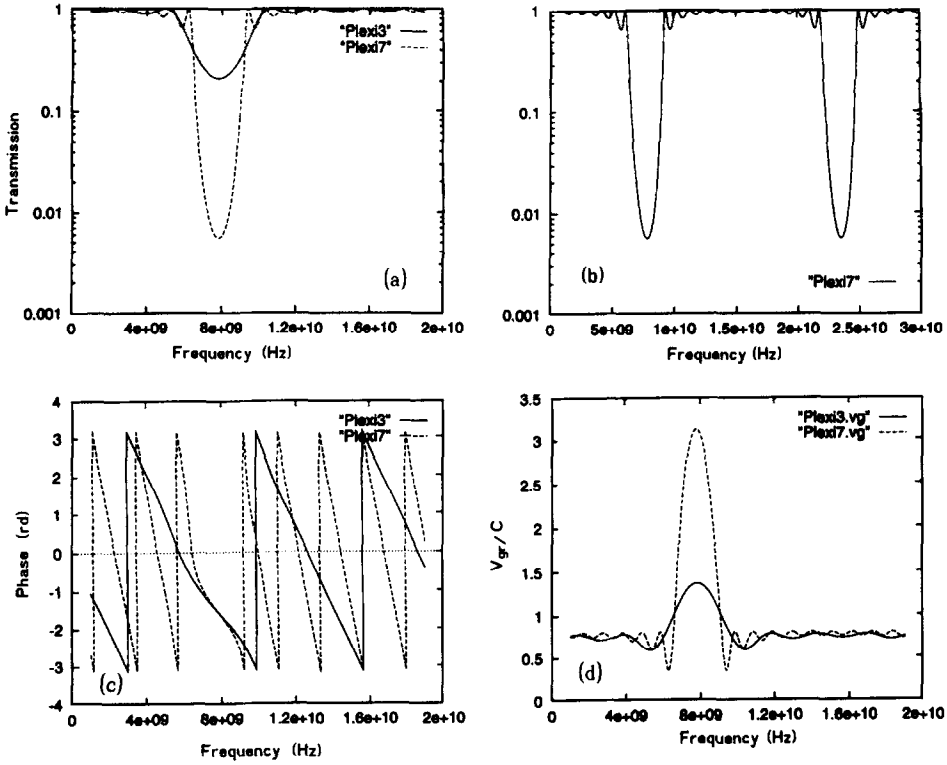

Fig. 4. (a) Transmission vs frequency of two periodic Plexiglas/air hetero-structures with three and with seven Plexiglas layers, (the air distance is 9.6 mm, the Plexiglas layers are 6 mm thick with $n = 1.6$), (b) transmission vs frequency of the structure with seven Plexiglas layers showing a second band gap, (c) phase shift vs frequency of the two structures, and (d) group velocity vs frequency of the two structures, the velocity is normalized to the vacuum velocity of light.

length. The arrival of the two signals were observed with an oscilloscope (HP 54124) with a time resolution ≤ 10 ps. It was found, that the tunneled signal has arrived 293 ps earlier than that which has travelled through the air. This result corresponds to a barrier traversal velocity of the signal of $4.34 \cdot c$.

Spielmann *et al.*[13] have measured the traversal time of periodic hetero-structures in the forbidden frequency regime with 12 fs long optical pulses of 375 THz. They found that the group velocities increase with barrier thickness in agreement with former microwave results.[29] In the 1960s Hartman predicted this effect for electrons.[14]

Another microwave experiment related to superluminal propagation of evanescent electromagnetic waves was carried out by Ranfagni *et al.*[12] They have studied the propagation of another type of evanescent microwave modes, the 'leaky waves' with two horn antennas as shown in Fig. 8, and have observed superluminal signal velocities.

3.2. *Single photon tunneling*

Tunneling through frequency band gaps of a dielectric heterostructure was studied at a single photon level by Steinberg *et al.*[11] The experimental set-up is presented in Fig. 9. In this experiment photon twins were generated by a down-conversion process in a KDP crystal. One of the two photons travelled through vacuum whereas the second one was sent through the barrier structure. The phase shift of the latter was shorter thus resulting in a travelling time through the barrier less than the time for the same distance in vacuum. Due to a correlation time of the twins of $\pm$ 20 fs, measurements of the interference distance had to

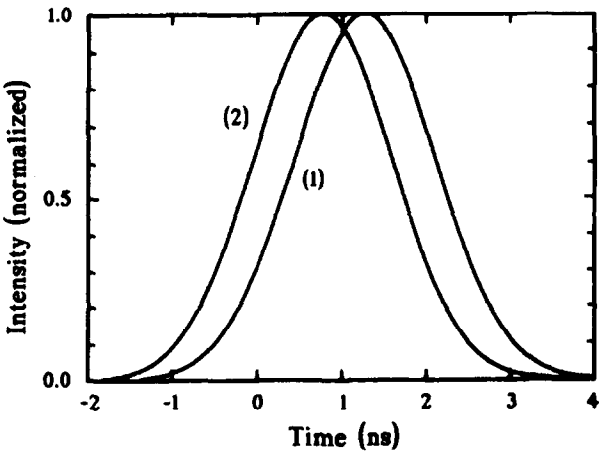

Fig. 5. Barrier traversal time of a microwave packet through a multilayer structure inside a waveguide. The center frequency of the pulse has been 8.7 GHz, the pulse width $\pm$ 0.5 GHz. The pulses are normalized. The maxima correspond to the center of mass and yield the group velocity. The barrier length was 114.2 mm. The group velocity of the tunneled signal was 4.7 c. The transmission of the barrier is shown in Fig. 3(b). The slow pulse (1) traversed the empty waveguide, whereas the fast one (2) has tunneled the forbidden band gap of the same length.

be averaged over some 20 million twins (the barrier crossing time being only 2.2 fs). This means that in this experiment an ensemble of many photons is necessary in order to determine the photon's barrier traversal time. Thus the claimed single photon experiment equals the microwave experiments from the physical point of view, where the same number of photons have been investigated in one pulse within some nanoseconds. In addition the detection process has been a quantum mechanical one in both experiments based on single photon–electron interaction. The difference is, that in the microwave experiments the tunneling events were elegantly counted within some ns, whereas in the single photon experiment the time of photon counting needs several hours.

Spieker[30] has shown that the experimental data of both investigations, the microwave and the single photon experiments, can be described quantitatively by assuming Gaussian wave packets and calculating the classical transmission function of the quarter wave layer periodic

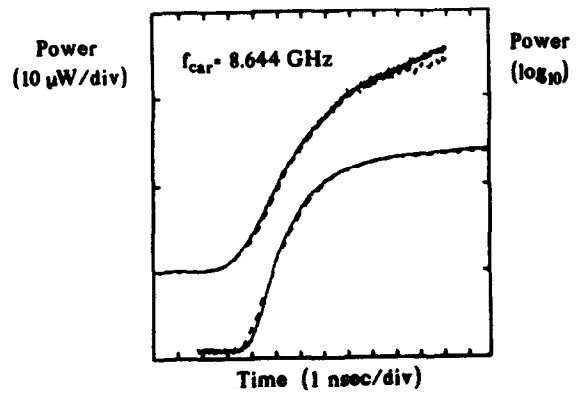

Fig. 6. Barrier traversal time of an amplitude modulated ramp. The carrier frequency of this signal has been 8.644 GHz and the cut-off frequency of the undersized wave guide (barrier height) 9.49 GHz. One signal has tunneled through a 60 mm barrier (dashed line) arriving at the same time, as the reference signal with the barrier completely taken out of the waveguide. (Left hand ordinate linear scale, right hand ordinate logarithmic scale using μW.)

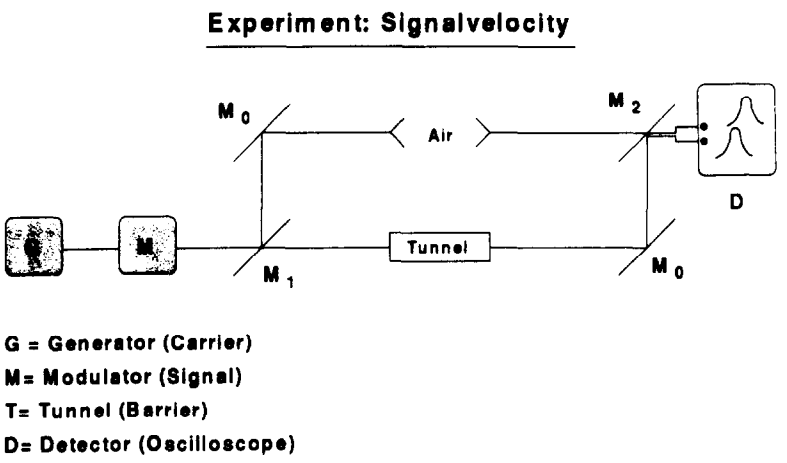

Fig. 7. Experimental set-up of a frequency band limited signal tunneling. The arrival of the tunneled signal is compared with the same signal traversed the same distance through air.

heterostructure. The computed absolute values and phase of the transmission function results in a transmission time in agreement with the experimental 'single photon' data.

3.3. *Resonant tunneling*

The analogy of the Helmholtz and the Schrödinger equations allows also to study resonant tunneling. Figure 10 shows a sketch of a microwave guide set-up with three resonant states in between two undersized waveguides forming the barriers.[22,31] The transition lines II and III have been analyzed. Both real and imaginary part of the transmission have been used to determine the linewidths. The decay time τ of the stored energy Q is related to the frequency ν according to $\tau = Q/2\pi\nu$. In electronics the resonant-state lifetime is often assumed to represent a time scale for the electron tunneling process.[4,8] The experiment has shown that the lifetime from the linewidth (real part of the transmission) agrees with the lifetime obtained

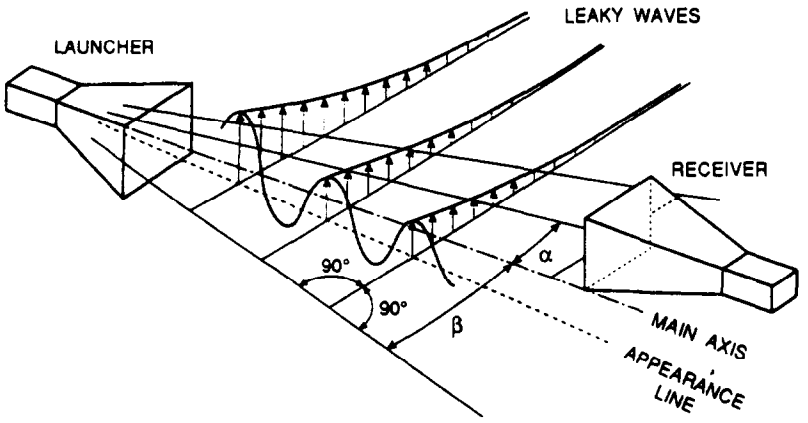

Fig. 8. Microwave propagation experiment with horn antennas. A special kind of evanescent waves, the leaky waves, is operating at moderate distances from the launcher and can be detected by the receiver in a selected range of values of the angle α. The leaky wave fronts are perpendicular to a plane nearly coincident with the vertical plane of the launcher horn, forming the angle β with the axis of the horn.[12]

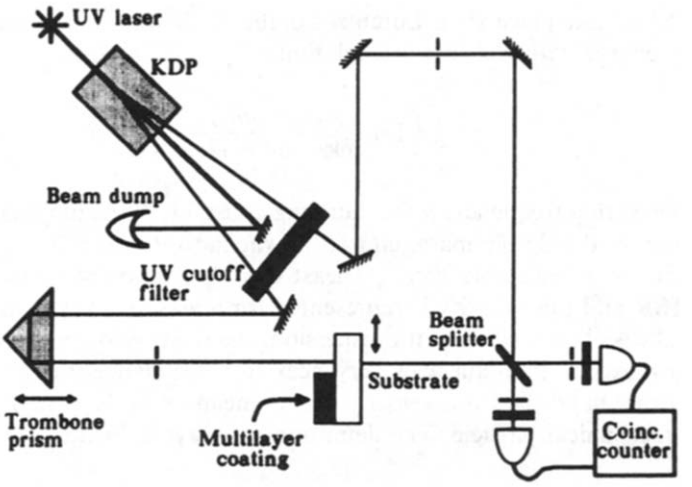

Fig. 9. Experimental set-up of the photon tunneling experiment[11]

from the derivative of the phase (imaginary part of the transmission). Compared with optical measurements, the microwave experiments have the important advantage of yielding both real and imaginary part of the transmission function. This allows the determination of the lifetime from two different experimental quantities. The lifetime of resonant line II is 40 ns, that of line III is 80 ns. We would like to point out that the resonant lifetime values are more than 2 orders of magnitude longer than the typical tunneling times for a single barrier. That means the resonant lifetime is not governed by the tunneling process.

3.4. *Tunneling with dissipation*

Experimental data on the tunneling time of charged particles such as electrons are rather difficult to interpret. Coulomb interactions with the environment are usually unavoidable and may even dominate the measured tunneling delay time. In order to take into consideration inelastic interactions the barrier may be represented by a complex potential as has been investigated theoretically.[32, 33] A complex tunneling barrier may be classically simulated with some restriction by a photonic barrier characterized by a complex refractive index.[34] Experiments with microwaves in undersized waveguides filled with a lossy dielectricum, i.e. the refractive index n being a complex number, have shown that dissipation is connected with an additional phase shift in the barrier region and accordingly with an increase of barrier traversal time. The superluminal barrier crossing disappears with increasing dissipation.[34] The experimental result has been predicted by the phase time calculations of Raciti and Salesi,[32] however, it has been opposite to the theoretical results from a path-integral solution of the telegrapher's equation by Mugnai *et al.*[33].

4. DATA ANALYSIS

4.1. *Definitions of wave velocities*

After the introduction of the theory of special relativity (TSR) by Einstein there has been much confusion about the very velocity which is not allowed to exceed the vacuum velocity of light. At that time Sommerfeld and Brillouin have defined the various velocities of waves and have explained the physics behind them.[35] The interaction of the electromagnetic waves

has been assumed to take place via a Lorentz–Lorenz oscillator, i.e. the waves interact with a bound electric charge with a dispersion relation

$$k^2 = \frac{\omega^2}{c^2}\left(1 + \frac{Ne^2/(m\epsilon_0)}{\omega_0^2 - \omega^2 - i2\omega\rho}\right).$$

where ω is the measuring frequency, ρ the damping constant, N the number of dipoles, e the elementary charge, m the dipole mass, and ϵ_0 the vacuum permeability.

It is the velocity of a detectable effect (at least one photon) or of an information, which counts for the TSR and this velocity is represented for a wave packet by the group velocity or in the classical case in a medium with dispersion, the front velocity. Both wave velocities never do exceed c except at frequencies very near to a resonance interaction as shown in Fig. 11. On the other hand the front velocity has no meaning in the case of a photon or any other quantum mechanical particle. The definition for wave velocities are

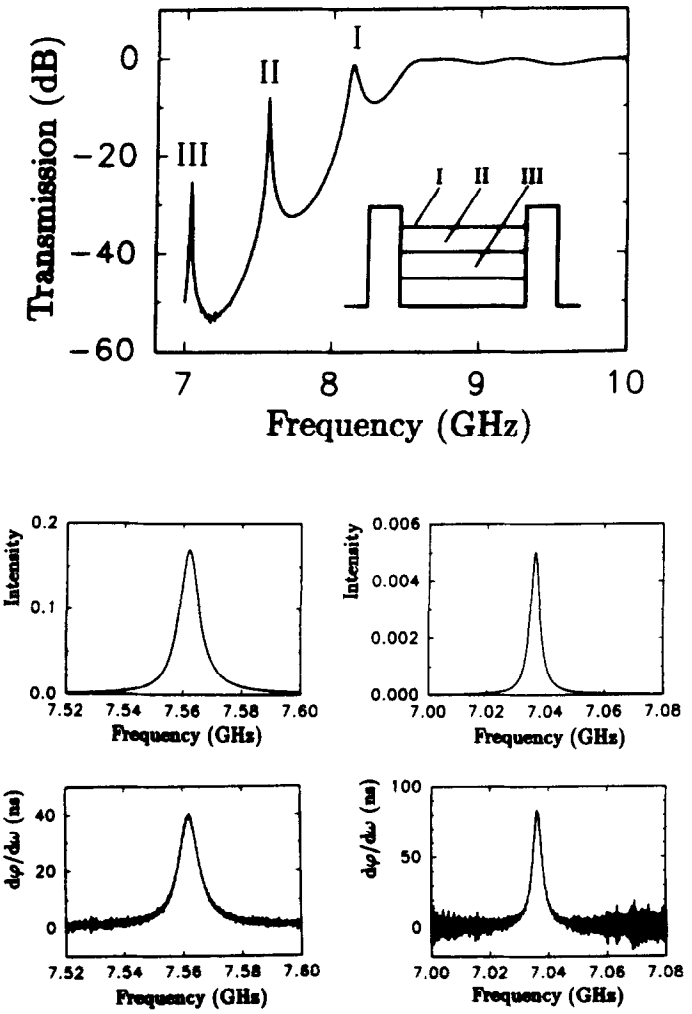

Fig. 10. Transmission of a double-barrier structure with three resonant transition lines below the barrier's cut-off frequency (insert). The figures (center) present the intensity vs frequency of the resonant lines and (bottom) the phase time $d\varphi/d\omega$ of lines II and III as a function of frequency.

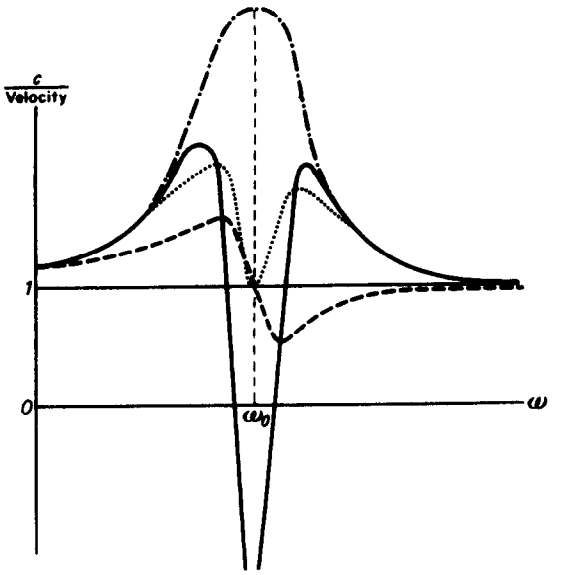

Fig. 11. Velocities vs frequency for electromagnetic waves in a dielectric medium described by a Lorentz–Lorenz dispersion. Key:-- -: c/v_{ph}, -: c/v_{gr},....:c/v_S,-.-.-.-: c/v_ϵ.[35]

Phase velocity	$v_{ph} = \omega/k$
Group velocity	$v_{gr} = d\omega/dk$
Front velocity	$v_F = \lim_{\omega\to\infty}\omega/k$
Signal (Information) velocity	$v_S \to v_F \geq v_S \geq v_{gr}$
Energy velocity	$v_\epsilon = \mathbf{S}/u$
Phase–time velocity	$v_\phi = z/(d\phi/d\omega)$

The velocities in a dielectric medium with a Lorentz–Lorenz dispersion are illustrated in Fig. 11.[35] Far from the resonance region the absorption is negligible and the imaginary part of the refractive index can be neglected. Here the group velocity represents the velocity of the signal as well as the velocity of the energy flow. However, near the resonance frequency the group velocity becomes greater than the velocity of light, can be infinite and even negative.

In this region the group velocity does no longer represent the velocity of a signal or of energy.[36, 37] In this region it is very difficult to define a signal velocity precisely, since the signal arrives very gradually without a distinct front. The absorbing situation near resonance has been experimentally and theoretically investigated, and it has been shown, that there was no conflict with the TSR.[37] In the case of reflection causing a finite standing wave ratio as in the case of the propagation of an evanescent mode the energy velocity lacks a physical meaning.

As long as we are dealing with waves, the interpretation of experimental results are understood on the basis of the Lorentz–Lorenz or more sophisticated interaction mechanisms. Such dispersion models for the propagation of waves, however, are *a priori* not relevant for the propagation of evanescent, i.e. tunneling, modes which have no real wavenumbers. We shall discuss this case in Section 6.

4.2. *Real signals are frequency band limited; has this fact implications?*

Theoreticians usually assume that signals have an unlimited frequency spectrum, which alone guarantees a well-defined signal front.[38] However, in practice signals have always a limited frequency band, an unlimited frequency band signal cannot be generated. Such limited frequency band AM signals are shown in Fig. 12. Signal (a) was sent through an optical fiber

distance of 9000 km to test the novel erbium-doped fiber amplifiers.[39] The carrier frequency was 2×10^{14} Hz, and the modulation bandwidth was limited to about 10^{10} Hz, i.e. the signal's frequency band is four orders of magnitude smaller than the carrier frequency. This type of signal has been tunneled at a superluminal speed without significant loss of information. The information is given by the number of digits. In this sample, for instance two, one, one etc., the information (signal) is given by the half-width of the individual signal. The information does not depend on the magnitude as seen from inspecting Fig. 13. Signal attenuation and signal magnitude have no influence on its velocity. Such an ill defined argument, that attenuation will guarantee causality in superluminal tunneling, has been presented by Spielmann *et al.*[13]

As shown in Fig. 12 (b) frequency limitation results in a non-causal Fourier representation of the signal. In this theoretical Fourier representation of a frequency band limited signal there exist signal components before the signal is switched on. This non-causal behaviour may hinder the theoretical description and an analysis of the experimental data.[40]

An often used argument in order not to violate causality is pulse or signal reshaping in consequence of the evanescent dispersion relation. High frequency components, if there are,

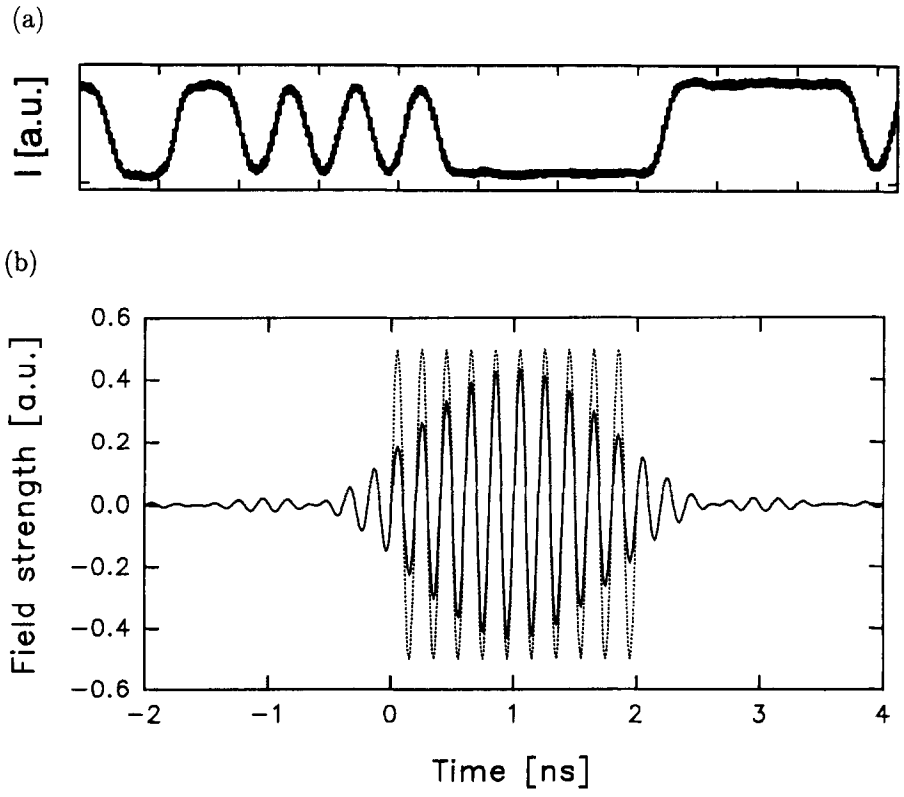

Fig. 12. (a) Signal used in optical fiber technology. The signal halfwidth corresponds to the number of bits, i.e. to the transmitted information. The abscissa is scaled in units of 1.5 ns. The carrier frequency is 2×10^{14} Hz and the amplitude modulation is limited to a band width of about 10^{10} Hz. (b) Sine wave signals non-frequency and frequency band limited (solid line 5 GHz $\pm$ 0.5 GHz). In consequence of the Fourier transform the frequency band limited signal has already signal components at negative times, i.e. before it is switched on.

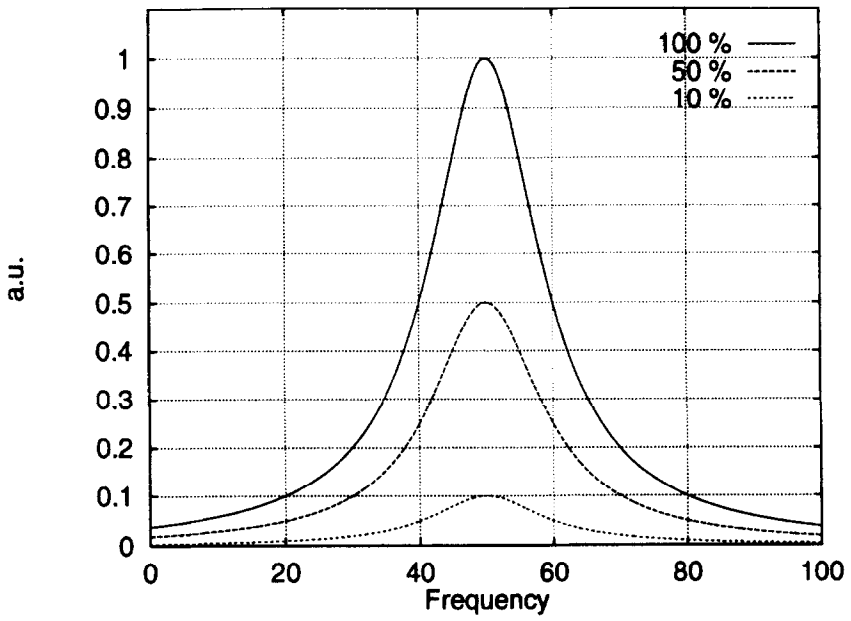

Fig. 13. Sketch showing that the half-width of a signal does not depend on its magnitude.

may be strongly favoured in the case of a single barrier dispersion (see dispersion relation of Fig. 3(c)). This would result in a pulse reshaping, in which the center of mass is shifted to the front of the signal. The situation is quite different in the case of a forbidden band gap in ordered heterostructures as displayed in Fig. 3(c), where the dispersion is rather symmetrical to the center frequency. However, pulse reshaping plays not a role in the case of the transmission of frequency band limited signals as has been discussed by Heitmann and Nimtz.[38]

We think, the fact that technical signals and all physical events are limited in their frequency spectrum represents an important point, which has not been given much attention to recently. In the following we shall discuss and present some results on the signal propagation of evanescent modes.[35, 34] A group of waves or a wave packet is a signal of finite length, comprising only of a limited number of frequencies. Whereas the phase velocity and the group velocity are well established quantities, the signal velocity v_s and the energy velocity v_E represent obviously fuzzy quantities. The problem of signal velocities has been treated in papers by Sommerfeld and by Brillouin, see Ref. 35. In order to investigate the wave propagation in a medium they assumed a signal given by the formula $f(t) = 0$ ($t < 0$ and $t > T$) and $f(t) = \sin(\omega_0 t)$ ($0 < t < T$) which is terminated at both ends, see Fig. 12(b). Such a wave form is composed of two unterminated waves, one beginning at $t = 0$ and the second at $t = T$ with opposite phase, so that the two cancel for all time $t > T$).

The Fourier analysis of this signal yields after several transformations

$$f(t) = \frac{1}{2\pi} \operatorname{Re} \int_{-\infty}^{+\infty} \left[e^{i\omega(t-T)} - e^{i\omega t} \right] \frac{d\omega}{\omega - \omega_0}.$$

If this signal traverses a distance z, each wave ω propagates with its phase velocity $v_{ph}(\omega)$ and the integral becomes

$$f(t,z) = \frac{1}{2\pi}\,\mathrm{Re}\int_{-\infty}^{+\infty}\left[e^{i\omega(t-T-z/v_{ph}(\omega))} - e^{i\omega(t-z/v_{ph}(\omega))}\right]\frac{d\omega}{\omega-\omega_0}.$$

In any dispersive medium the highest frequency components will arrive at z with c. They do not interact with the medium and their weak oscillations are called forerunners or front. At a lower speed the main signal will arrive, which will be deformed. If it is possible to determine the exact moment when this main signal arrives, this defines the signal velocity. One has to distinguish between the wave front velocity, which might be determined by a forerunner, and the colloquial signal velocity, with which the main part of the wave propagates in a dispersive medium. In general, the signal velocity measured depends on the sensitivity of the detecting apparatus used. With a very sensitive detector, even the forerunners might be detected.[41] Only if the detector is restricted to a quarter or to all of the final signal intensity, then an unambiguous definition of the signal velocity can, in general, be given.[35]

If we are not dealing with a signal with a sudden start and a sudden ending (the realistic and the only procedure signals and reactions are mediated) we can suppress frequencies very different from ω_o and the formula becomes by expansion of the exponents

$$f(t,z) = \frac{1}{2\pi}\,\mathrm{Re}\left\{e^{i\omega_0(t-z/v_{ph}(\omega))}\int_{\omega_0-\Delta\omega}^{\omega_0+\Delta\omega}\left[e^{i(\omega-\omega_0)(t-T-z/v_{gr}(\omega_0))} - e^{i(\omega-\omega_0)(t-z/v_{gr}(\omega_0))}\right]\frac{d\omega}{\omega-\omega_0}\right\}.$$

This equation represents a signal beginning progressively at $t = 0$ and arriving at z at a time $t = z/v_{gr}$, ending at $t = T$ and $t = T + z/v_{gr}$, respectively. The velocity of the wave front is now equal to the group velocity $v_{gr}(\omega_0)$.

Assuming an evanescent medium having a purely imaginary wave number κ, which is independent of frequency in the range $\omega_0 \pm \Delta\omega$ it follows

$$f(t,z) = \frac{1}{2\pi}e^{-\kappa z}\mathrm{Re}\left\{e^{i\omega_0 t}\int_{\omega-\omega_0}^{\omega-\omega_0}\left[e^{i(\omega-\omega_0)(t-T)} - e^{i(\omega-\omega_0)t}\right]\frac{d\omega}{\omega-\omega_0}\right\}.$$

This limited frequency band signal decays exponentially at traversing the distance z, however, without spending any time in the evanescent region. Even the rising edge of the signal propagates with the group velocity, however fast it may become in traversing the evanescent region. A surprising result, which, however, is in agreement with the experimental data. The evanescent frequency components of a signal do not spent time in the evanescent region. The observed time delay is due to the phase shift at the barrier boundary.

4.3. *Superluminal tunneling and the Hartman effect*

With the first electronic tunneling experiments in solid state physics the important question arose, how much time will the electron spent in the barrier region? Hartman carried out the first quantitative phase time calculations.[14] Using the time dependent Schrödinger equation, he has calculated the traversal time of Gaussian wave packets tunneling through rectangular potential barriers. The normalized data are shown in the graphs of Fig. 14. For thin barriers the calculated transmission time of the peak of the wave packet is longer than the equal time, i.e. the corresponding vacuum time. With increasing barrier length, however, the transmission time becomes constant and less than the equal time. Above the crossover of the two functions the group velocity of the tunneled particle exceeds the vacuum velocity, i.e. the particle velocity in the case of the photons becomes superluminal. This effect is often called Hartman effect and has been experimentally confirmed for the first time with microwaves by Enders and Nimtz.[29] The dots in the same figure are values measured with evanescent microwaves in undersized waveguides of various lengths. Also in an optical experiment with a periodic

dielectric heterostructure the dependence on the evanescent region length of the transmission time has been observed by Spielmann *et al.*[13]

4.4. *Tunneling vs resonant tunneling*

Previously several attempts were made to obtain information on the electronic barrier transition time from the line width of a resonant tunneling state e.g. Ref. 8. The photonic data from both amplitude and phase measurements have shown (see Section 3.3) that the line width corresponds to the time the electromagnetic wave packet spends between the two barriers. This time is much larger than the measured single barrier transition time (see Section 3.1), and does not contain any information on the latter. The measured resonant photonic tunneling time is also in fair agreement with the historical quantum mechanical approach to describe a nucleus decay by Gamov. This agreement also points on the analogy of the Helmholtz equation and quantum mechanics.

5. APPROACHES TO THE TUNNEL TIME

How much time does a (quantum mechanical) particle need to travel through a classically forbidden region of space, i.e. when its kinetic energy is less than the potential?

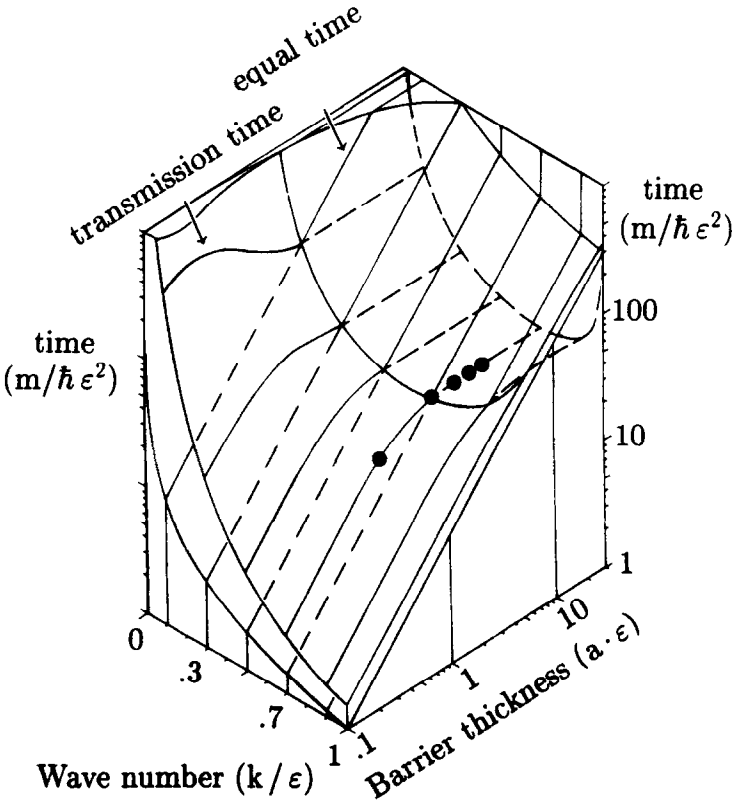

Fig. 14. Graphs of the calculated particle transmission time as a function of barrier thickness.[14] Where m is the particle mass, $\hbar$ the Planck constant, and k/ϵ is the incident wave number normalized to ϵ, the wave number equivalent to the potential barrier height. The dots represent the appropriately scaled experimental data of transmission time of evanescent electromagnetic waves. Experimental parameters are as follows: center frequency of the Guassian-like wave packet $\nu = 8.7$ GHz, barrier length 10, 40, 60, 80, 100 mm, for more details see Ref. 29.

There have been a lot of attempts to answer this question, none of which is regarded as the definite solution. In the past decade this question became an active and fashionable subject, last not least stimulated by recent experiments. There are already a number of reviews on the tunnel time problem, three of which are the most often cited: one by Landauer and Martin,[6] a somewhat older by Hauge and Støvneng[4] and an interim one by Olkhovsky and Recami.[5] A list of literature including also very recent articles is given with full title and a very short summary of the main result in.[42]

Many, though not all of the approaches fit into three categories. One might follow wave packets incident on the barrier, passing through it, and compare a feature of the transmitted and incident wave packet. Another method is to determine a set of dynamic paths $z(t)$, calculate the time a path spends in the barrier and, may be, average over all these times. Last not least, one tries to attach a physical clock to the particle and determine the time elapsed during tunneling. The following sections present introductions to these approaches.

5.1. *Wave packets*

Wave packets have been a very successful tool in describing the propagation of particles and in accounting for the uncertainty in the experimental observables. The most probable measured values are given at the maximum of the wave packet, i.e. its probability amplitude. This can be determined when the initial, reflected and transmitted wave packets are far away from the barrier so that there is no disturbance due to interference effects. If there was no barrier one would know the non-influenced propagation behaviour. Propagation of the wave packets with this behaviour to the beginning ($z = 0$) and to the end ($z = d$) of the barrier allows to determine times for the maxima $t_I(0)$, $t_R(0)$, $t_T(d)$. That is a non-invasive asymptotic method, which takes effort to realize in experiments. So done, the transmission and the reflection time are $\tau_T(0,d) = t_T(d) - t_I(0)$ and $\tau_R(0,d) = t_R(0) - t_I(0)$. In the plane-wave limit, i.e. narrow wave packets in k-space, these times become in the case of electrons:

$$\tau_T^{\varphi}(k_0,0,d) = \frac{d}{\hbar k_0/m} + \hbar \frac{\partial \varphi_T}{\partial E}\Big|_{k_0}$$

the phases given by

$$T = |T|e^{i\omega_T}\tau_R^{\varphi}(k_0,0,d) = \hbar \frac{\partial \varphi_R}{\partial E}\Big|_{k_0} R = |R|e^{i\varphi_R}$$

Hartman[14] has plotted the transmission time versus the particle energy and the barrier length (see Fig. 14).

In the case of microwaves in the Cologne experiment,[9, 20] of laser pulses in the Vienna experiment[13] and of photons in the Berkeley experiment[43] the same method can be applied to the electromagnetic field. One can prove that $d/\tau_T = v_{Gr} = d\omega/dk|\omega_0$ holds, the right part making sense when $k(\omega_0) \in \mathbb{R}$. The experimentally and theoretically obtained times agree within the experimental errors.

There are some interpretational difficulties with the wave packet approach. Landauer and Martin[44] criticized that there is no justification for assuming that the centroid of the incident packet evolves into the centroid of the transmitted and reflected packets. They argue that due to the dispersive propagation of the packet the high-energy components would reach the barrier first. Since they are more effectively transmitted, the transmitted packet comes from the 'front' of the incident packet, may be, leaving the barrier long before the centroid of the incident packet has arrived. This process is called pulse reshaping. In the photonic case there is no such dispersion in free space. Doesn't the Fourier theorem tell us that all energy components are spread evenly over the whole wave packet (and 'beyond')? Neither phase velocity nor group velocity may be used in the former interpretation. This argument applies also to the dispersion *inside* the tunnel region.

It is observed that the group velocity becomes superluminal when the main frequency component and most of the supporting frequency band is in the 'tunnel' regime, i.e. where there is little transmission, $|T(\omega)| \ll 1$. Though there is strong damping, it is astonishing to see in numerical simulations[45] that the transmitted wave packet has almost the same shape (less than one per thousand deviation) as the incident one as long the frequency support is not too broad and the barrier is not too long.

Superluminal group velocities raised the problem of causality. It is stated by Heitmann and Nimtz[38] that only the front velocity[1] has to obey Einstein causality which is, however, an ambiguously measurable quantity. This agrees with a demand for the Green's function being zero before d/c.[48] An analytic expression of Green's function for the microwave experiment without the use of advanced solutions was given recently by Emig.[45]

5.2. *Paths*

There are several possibilities for defining particle trajectories. This is a delicate picture in quantum mechanics as the particle position and momentum obey the Heisenberg uncertainty relation. Thus a classical trajectory does not exist.

5.2.1. *Bohm view*. A very good introduction and treatment is given by Leavens and Aers[49] of which a short summary is presented here.

In Bohm's interpretation of non-relativistic quantum mechanics an electron *is* a particle, the motion of which is causally determined by an objectively real complex-valued field $\psi(z,t)$ so that it has a well defined position and velocity at each instant of time. The guiding field

$$\psi(z,t) = R(z,t)e^{\frac{i}{\hbar}S(z,t)} \quad R,S \in \mathbb{R}$$

satisfies the time dependent Schrödinger equation. $R^2(z,t) \equiv |\psi(z,t)|^2 \equiv P(z,t)$ is the probability density for an electron for *being* at position z at time t. $S(z,t)$ satisfies the Hamilton–Jacobi equation

$$\frac{\partial S}{\partial z}\Big|_{z,t} + \frac{1}{2m}\left(\frac{\partial S}{\partial z}\Big|_{z,t}\right)^2 + V(z,t) + Q(z,t) = 0$$

with the quantum potential

$$Q(z,t) \equiv \frac{\hbar^2}{2m}\frac{1}{R}\frac{\partial^2 R}{\partial z^2}.$$

The velocity is defined by

$$v(z,t) = \frac{1}{m}\frac{\partial S}{\partial z}$$

and satisfies

$$v(z,t) = \frac{j(z,t)}{P(z,t)} \equiv \frac{1}{|\psi(z,t)|^2}\frac{\hbar}{2im}\left[\psi^*(z,t)\frac{\partial \psi}{\partial z}\Big|_{z,t} - \psi(z,t)\frac{\partial \psi^*}{\partial z}\Big|_{z,t}\right]$$

[1] If one introduces a front into the incident wave packet, one finds, that this always travels with the speed of light in vacuum c [http://www.uni-koeln.de/ ~ abb11/cs.ps.gz]. Numerical simulations were carried out with such a step and an analytic continuation on zero-level. Simulations show too, that the velocity of the maximum also depends on the width of the wave packet.[46,47]

which is the *net* probability flux divided by the probability density. Given the initial position $z_0 \equiv z(t = 0)$ of an electron with the initial wave function $\psi(z,t = 0)$, its subsequent trajectory $z(z_0,t)$ is uniquely determined by simultaneous integration of the time dependent Schrödinger equation and the guidance equation $dz/dt = v(z,t)$. It is a feature of these trajectories that they do not intersect.

The time spent in the region $z_1 \leq z \leq z_2$ is unambiguously given by

$$t(z_0;z,z_2) = \int_0^\infty dt\, \Theta[z(z_0,t) - z_1]\Theta[z_2 - z(z_0,t)]$$

accounting for multiple passes through this region. The mean dwell time is the statistical average over these times with the probability distribution of the initial position $P(z_0,t)$

$$\tau_D(z,z_2) \equiv \int_{-\infty}^{\infty} dz_0\, P(z_0,0)\, t(z_0;z_1,z_2) = \int_{z_1}^{z_2} dz\, |\psi(z,t)|^2$$

Since Bohm trajectories do not intersect each other there exists in the case of a barrier a special starting point z_{0C} given by

$$\int_{z_{0C}}^{\infty} dz\, |\psi(z_0,t)|^2 = |T|^2$$

such that only those trajectories $z(z_0,t)$ with $z_0 > z_{0C}$ are ultimately transmitted through the barrier contributing to $|T|^2$ and only those with $z_0 < z_{0C}$ are ultimately reflected from the barrier contributing to $|R|^2$. Hence the mean transmission and reflection times are uniquely given by

$$\tau_T(z_1,z_2) = \frac{1}{|T|^2} \int_{z_{0C}}^{\infty} dz_0\, P(z_0,0)\, t(z_0;z_1z_2) \in \mathbb{R}^+$$

$$\tau_R(z_1,z_2) = \frac{1}{|R|^2} \int_{-\infty}^{z_{0C}} dz_0\, P(z_0,0)\, t(z_0;z_1,z_2) \in R^+$$

and the sum rule

$$\tau_D = |T|^2\tau_T + |R|^2\tau_R$$

holds. It is remarked that there are trajectories contributing to $|R|^2$ which do not enter the barrier region.

A surprising fact at first glance is that the transmitted part of a coherent sum of incident wave packets following each other in the initial wave function may emerge from the first wave packet only.

A similar approach for photons might be based on the *instant* energy velocity of the electromagnetic field[47] though the problem of interpreting the energy density as a probability density occurs.[50] Instead, trajectories for the field *configuration* can be determined.[51]

The Bohm approach intrinsically yields traversal time distributions.[49] The mean times determined by averaging are substantially longer than those of the clock approaches. Since in the Bohm approach the velocity is always less than c there is no causality problem. Corresponding time measurements were attempted. The Berkeley experiment gives a time distribution which does not agree with this approach.[47] A severe criticism is, that the

trajectories are not covariant even for the underlying wave equations that are relativistically invariant.

5.2.2. *Path integrals*. The Feynman path integral techniques were used by Sokolovski and coworkers[52-54] for the determination of propagation times. For a classical path $z(t)$ the time spent in the region $z_1 \leq z \leq z_2$ is

$$t[z_1,z_2;z(t)] = \int_0^\infty dt\, \Theta[z(t) - z_1]\, \Theta[z_2 - z(t)].$$

A dwell time is defined by substituting $z(t)$ with a Feynman path $z_F(t)$ and averaging with the weight factor $e^{i/\hbar\, S[z_F(t)]}$ for action S over all the paths joining spacetime points $(z_0,0)$ and (z_∞,t_∞) with $z_0 \leq z_1$ and $z_\infty \geq z_2$

$$\tau_D(z_1,z_2) = \frac{\displaystyle\int_{z_0}^{z_\infty} Dz_F(t')\, t[z_1,z_2;z_F(t')]\, e^{\frac{i}{\hbar} S[z_F(t')]}}{\displaystyle\int_{z_0}^{z_\infty} Dz_F(t')\, e^{\frac{i}{\hbar} S[z_F(t')]}}$$

using functional integration. In terms of quantum mechanical states this is

$$\tau_D(z_1,z_2) = \frac{\langle \psi^*(z_\infty,t_\infty)\, t[z_1,z_2;z_F]\, \psi(z_0,0)\rangle_F}{\langle \psi^*(z_\infty,t_\infty)\, \psi(z_0,0)\rangle_F}$$

which again evaluates to

$$\tau_D(z_1,z_2) = \int_0^\infty dt \int_{z_1}^{z_2} dz\, |\psi(z,t)|^2.$$

In the plane-wave limit with wavenumber k_0 and probability current $\hbar k_0/m$ this is

$$\tau_D(k_0;z_1,z_2) = \frac{1}{\hbar k_0/m} \int_{z_1}^{z_2} dz\, |\psi_{k_0}(z,t)|^2$$

which was also given by Büttiker.[55] The transmission and reflection times are introduced by decomposition of the wavefunction at sufficiently large times t_∞ into these parts, i.e. $\psi(z_\infty,t_\infty) = \psi_T(z_\infty,t_\infty) + \psi_R(z_\infty,t_\infty)$. In the above limit Sokolovski and Baskin find

$$\tau_T^{SB}(k_0;z_1,z_2) = i\hbar \int_{z_1}^{z_2} dz\, \frac{\delta \ln T(k_0)}{\delta V(z)} \in \mathbb{C} \qquad T = |T| e^{i\varphi_T}$$

with

$$\tau_R^{SB}(k_0;z_1,z_2) = i\hbar \int_{z_1}^{z_2} dz\, \frac{\delta \ln R(k_0)}{\delta V(z)} \in \mathbb{C} \qquad R = |R| e^{i\varphi_R}$$

and obeying the sum rule

$$\tau_D^{SB} = |T|^2 \tau_T^{SB} + |R|^2 \tau_R^{SB} \in \mathbb{R}$$

The problem that occurs here are τ_T^{SB} and τ_R^{SB} being complex and it was questioned what the real time is. This problem will be picked up later.

5.2.3. *Wigner function.* The last path concept presented here uses the Wigner function, introduced by Wigner.[56] Such trajectories were first calculated by Lee and Scully[57] and recently discussed for the tunnel problem by Marinov and Segev.[58] The Wigner function is defined in phase space by

$$W(q,p,t) = \frac{1}{\pi\hbar}\int_{-\infty}^{\infty} dz e^{-i2p/\hbar}\psi^*(q-z,t)\psi(q+z,t)$$

If the third and higher-orders of the potential vanish, the Wigner trajectories coincide with the classical paths. Otherwise the Wigner trajectories are defined with a modified 'quantum' potential and are not classical. For a system in an energy eigenstate (i.e. in the stationary barrier problem), the time-shift invariance implies that the trajectories are 'equi-Wigner curves' which are lines of constant value of the Wigner function. The 'effective' potential may be singular, the Liouville theorem is violated, and quantum jumps can hardly be included. Once trajectories are found, the transmission time is calculated the same way as in Bohm's approach. The weighting with the initial distribution $W(q_0,p_0,0)$ may involve negative probabilities.

5.3. *Clocks*

There are various attempts to find transmission times with techniques of standard quantum mechanics. The Larmor clock is of intrinsic type whereas the Quantum clock is an extrinsic one, i.e. the latter influences the wavefunction. How can the wavefunction be decomposed in to-be-transmitted and to-be-reflected parts? One possibility is to analyze the probability flux and another one is to use projection operators. Though some results are recovered, up to now, no method can be fully justified and be regarded as the definite solution.

5.3.1. *Larmor clock.* The real and the imaginary parts of $\tau_T^{SB}(k_0;0,d)$ are identical to the spin-precession traversal time of Rybachenko[59] and the spin-rotation traversal time of Büttiker,[55] respectively. These are derived, following Baz',[60] from an analysis of the effect of an infinitesimal uniform magnetic field, confined to the barrier, on the components of the average spin per transmitted electron in the plane perpendicular to the field (Larmor effect) and in the field direction (Zeeman effect), respectively. The same method was applied to the Faraday rotation of the electromagnetic field polarization in the optical case by Gasparian[61] and its realization in an experiment was proposed by Deutsch and Golub,[62] of which the result is yet missing. The spin-precession traversal time is independent of the width d of an opaque barrier leading again to a mean transmission speed that can exceed c even in the corresponding relativistic calculation.[63] The spin-rotation can be negative for the above barrier transmission. To avoid these problems Büttiker introduced $|\tau_T^{SB}(k_0;0,d)| \in \mathbb{R}^+$ which is identical to the Büttiker–Landauer traversal time derived by considering a time-modulated barrier[64] (see below). A recent analysis shows that the Larmor clock reading *during* the tunnel process depends on time and on the width of the wave packets[65] and may run backwards.

5.3.2. *Quantum clock.* A quantum mechanical clock with discrete time readings, i.e. states, was introduced by Salecker and Wigner[66] and applied to tunneling through a barrier by Leavens and McKinnon.[67] Let $u_m(\theta)$ $(m = -1,0,1)$ be the eigenfunctions of a clock Hamiltonian $\hat{H}_C$ and let

$$v_n(\theta) = \frac{1}{\sqrt{3}}\sum_{m=-1}^{1} e^{i2\pi nm/3}u_m(\theta) \quad (n = 0,1,2)$$

be the eigenfunctions of a clock-time operator $\hat{T}_C$ with a time resolution τ. The total system Hamiltonian is

$$\hat{H} = -\frac{\hbar^2}{2m}\frac{\partial^2}{\partial z^2} + V(z) + \Theta(z - z_1)\,\Theta(z_2 - z)\,\hat{H}_C$$

such that the clock only runs inside the region $z_1 \leq z \leq z_2$. The dwell time becomes

$$\tau_D^{SW}(0,d;E) = \frac{\hbar}{V_0}\sqrt{\frac{E}{V_0 - E}}$$

for an opaque rectangular barrier ($\kappa d \gg 1$). One must take care that the perturbation of the particle by the clock is negligible. The calibrated Salecker–Wigner clock results give the widely accepted dwell time $\tau_D(k_0;z_1,z_2)$, a possibly superluminal tunnel transmission time $\tau_T(k_0;z_1,z_2)$ and a negative tunnel reflection time $\tau_R(k_0;z_1,z_2)$.

5.3.3. *Probability current.* A conventional probability current density approach was discussed by Olkhovsky and Recami[5] and by Muga *et al.*[68] Splitting up the probability current $J(z,t) = J_+(z,t) + J_-(z,t)$ allows one to define times

$$\tau_T^J(0,d) = \frac{\int_0^\infty dt\, t\, J_+(d,t)}{\int_0^\infty dt\, J_+(d,t)} - \frac{\int_0^\infty dt\, t\, J_+(0,t)}{\int_0^\infty dt\, J_+(0,t)}$$

$$\tau_R^J(0,d) = \frac{\int_0^\infty dt\, t\, J_-(0,t)}{\int_0^\infty dt\, J_-(0,t)} - \frac{\int_0^\infty dt\, t\, J_+(0,t)}{\int_0^\infty dt\, J_+(0,t)}.$$

One could choose

$$J_+(z,t) = J(z,t)\,\Theta[J(z,t)] \qquad J_+(z,t) = \int_0^\infty dp\,\frac{p}{m}\,\tilde{J}(p;z,t)$$

or

$$J_-(z,t) = J(z,t)\,\Theta[-J(z,t)] \qquad J_-(z,t) = \int_{-\infty}^0 dp\,\frac{p}{m}\,\tilde{J}(p;z,t)$$

with either sorting for the sign of the total current or for the sign of the contributing momenta to the current. The problems are that $J = J_+ + J_-$ is not unique and that a decomposition $J_\pm = J_{\pm,T} + J_{\pm,R}$ is not possible. Also τ_T^J can be negative.

5.3.4. *Projectors.* It was suggested by Brouard *et al.*[69] to use operators for identifying components of the wavefunction. Defining $\hat{D}(z_1,z_2)\,\psi(z,t) \equiv \Theta(z - z_1)\,\Theta(z_2 - z)\,\psi(z,t)$ leads again to

$$\tau_D(z_1,z_2) = \int_0^\infty dt \int_{-\infty}^\infty dz\, \psi^*(z,t)\,\hat{D}(z_1,z_2)\,\psi(z,t).$$

If it were possible to define $\hat{T}(z_1,z_2)\psi(z,t) \equiv \psi_T(z,t)$ and $\hat{R}(z_1,z_2)\psi(z,t) \equiv \psi_R(z,t)$ with $\hat{T} + \hat{R} = \hat{1}$ one could write

$$\hat{D} = \begin{cases} \hat{1}\hat{D} = \hat{T}\hat{D} + \hat{R}\hat{D} \\ \hat{D}\hat{1} = \hat{D}\hat{T} + \hat{D}\hat{R} \end{cases}$$

But $\hat{T}$ and $\hat{R}$ do not commute with $\hat{D}$. In general we have $\hat{D} = F(\hat{T},\hat{D}) + F(\hat{R},\hat{D}) + G(\hat{T},\hat{R},\hat{D})$ giving

$$\tau_D = |T|^2\tau_T^F + |R|^2\tau_R^F + \tau_{TR}^G$$

with

$$\tau_T^F(z_1,z_2) \equiv \frac{1}{|T|^2}\int_0^\infty dt \int_{-\infty}^\infty dz\, \psi^*(z,t)\, F(\hat{T},\hat{D})\, \psi(z,t)$$

$$\tau_{TR}^G(z_1,z_2) \equiv \int_0^\infty dt \int_{-\infty}^\infty dz\, \psi^*(z,t)\, G(\hat{T},\hat{R},\hat{D})\, \psi(z,t).$$

One observes that e.g. in the first order

$$\tau_T^{TD}(z_1,z_2) = \frac{1}{|T|^2}\int_0^\infty dt \int_{-\infty}^\infty dz\, \psi_T^*(z,t)\, \psi(z,t)$$

is identical to the Feynman path integral result.[53] Other expansions of $\hat{D}$ lead to transmission times which reproduce a lot of previous results using different approaches.

The systematic projector approach always does a wave-like decomposition of the wavefunction $\psi = \psi_T + \psi_R$ and is fundamentally incompatible with the Bohm trajectory approach which does a particle-like decomposition $|\psi|^2 = |\psi|_T^2 + |\psi|_R^2$.

5.3.5. *Modulated barrier and uncertainty.* A sort of external probing for finding the tunnel time was suggested by Büttiker and Landauer.[64] The original static barrier is augmented with small temporal oscillations in the barrier height, the amplitude of which are kept as small as desired. The incident particle sees an effective static barrier at low frequencies or is affected by a substantial part of the cycle(s) at high frequencies. The frequency at which the deviation from the adiabatic approximation occurs is an indication of the length of the time that a particle interacts with the barrier. It is not the eigenvalue of a Hamiltonian, indicative of a precisely measurable value. The characteristic traversal time for the (modulated) opaque rectangular barrier of length d is

$$\tau^{MB} = \frac{dm}{\hbar\kappa}$$

where $\hbar\kappa$ is the magnitude of the imaginary momentum under the barrier. A desirable feature is the proportionality of this time to the barrier length.

This result coincides with that of the approach by Hagman[70] who considers a particle tunneling through a rectangular barrier as *borrowing* an energy ΔE, to be able to cross the barrier with a real velocity, in time Δt. The minimum value of $\Delta E\Delta t$ is given by the Heisenberg uncertainty relation.

6. CONSEQUENCES FOR QUANTUM ELECTRONICS

Several microelectronic devices are based on the electronic tunneling process. The classical tunneling diode explained first by Esaki[2] consists of a p–n junction in which both p and n sides are degenerate (i.e. heavily doped with impurities). Because of the high dopings the Fermi level is located within the allowed bands themselves and causes a depletion-layer width only of the order of 10 nm. This distance corresponds to the potential barrier width the electrons have to tunnel from the conduction band on the n side to the valence band on the p side of the junction.[71]

Currently available semiconductor fabrication technology allowed the introduction of a double-barrier structure for resonant tunneling.[71] The photonic tunneling results are in agreement with the predictions of quantum mechanics. Thus we conclude, that the intrinsic tunneling time for electrons will also be determined by the available quantum mechanical calculations. That means, the utmost dynamical specification of a device can be calculated and only extrinsic influences due to interactions of the electrons with lattice defects and impurities in the device have to be determined.

7. VIOLATION OF CAUSALITY?

The question whether a superluminal photonic barrier transition violates causality has never been raised in the experimental papers by Enders and Nimtz.[9, 10, 29, 22, 31, 34] However, the superluminal results have provoked many theoretical studies (see Section 5) and discussions in several journals, even in newspapers and TV, e.g.[7, 15]. Reading all these contributions we came to the conclusion that most of the investigations and the arguments presented in the discussions are not related to the problem and have still not given an answer to the question whether the measured superluminal velocities do violate or not the causality or the theory of special relativity (TSR), see e.g.[38] In the following we shall present some of the new and strange experimental results, which we think have not been properly considered in the theoretical investigations so far.

7.1. *Back-in time communication?*

All signals generated and transmitted to a receiver are frequency band limited. For instance the frequency necessary to transmit music or language is of the order of 10 kHz. With the fiber optic systems signals are modulated up to the GHz-regime on a carrier with a frequency of 2×10^{14} GHz. A frequency band limitation results in a non-causal behaviour as demonstrated in Fig. 12(b). In addition frequency band limited signals do not have a front as discussed, see e.g.[40].

According to the Fourier presentation such a signal has already wave components at negative times, a well-known phenomenon.[40] As has been shown in various amplitude modulated signal experiments the signal can move faster than c. Even if it has been attenuated by several orders of magnitude, of course not beyond the noise level, the signal (i.e. the information) has been almost the same. We may conclude from the microwave experiments that back-in time communication can be realized. A second signal sent some time after the first one, can arrive at an observer earlier, when sent through a tunnel.

Recently Landauer[72] gave the following comment: *Are we quite sure that if we signal with photon polarization, and if we are willing to lose most of the photons in the evanescent region, that we have no chance of rare superluminal signal propagation*?

Aichmann *et al.*[73] have transmitted Mozart's 40th symphony through a barrier at a speed of $4.7 \cdot c$ in order to listen, whether this frequency band limited signal has experienced significant distortions, no distortion has been heard.

7.2. *Pulse reshaping and photon detectors*

Pulse reshaping is negligible as long as the signal band width is much smaller than the carrier frequency (see Section 5). This has been the case in the microwave experiments. Pulse reshaping has been suggested in several theoretical studies in order to preserve the TSR. This mechanism has been named also to explain causality for the single photon experiment by Steinberg *et al.*[11] The center of mass of the photon was assumed to have moved superluminally and shifted to the front, the latter, however, moved only with the velocity of light. In the case of single photon detection this argument is naive and not correct, because a detector measures the photon quantum and is not sensitive to a photon front. The front of a wave packet is without physical meaning in quantum mechanics.

7.3. *Superluminal energy transport*

Superluminal energy transport has been measured in several experiments. This fact has become most obvious in the single photon experiment, where the detector measured the presence of the photons energy.

The relation for the energy velocity $\overline{v_e} = \overline{P}/\rho$ with $\overline{P}$ the energy flux and ρ the energy density has a special meaning in the case that reflection occurs. In fact reflection takes place in the case of the propagation of evanescent modes, and it is the cause for the exponential decay of the evanescent mode. For example we investigate the one-dimensional case with $\overline{P_{inc}}$ and $\overline{P_{refl}}$ the incident and the reflected energy flux, respectively, and with $\overline{v_{e,M}}$ the energy velocity in the medium without reflection and dissipation. At some point of the transmission line reflection of flux $\overline{P_{refl}}$ occurs. The value is described by the reflection coefficient r, i.e. $\overline{P_{trans}} = \overline{P_{inc}} + \overline{P_{refl}} = (1 - r^2)\overline{P_{inc}}$ while $\rho = \rho_{inc} + \rho_{refl} = (1 + r^2)\rho_{inc}$ holds. The relation yields an effective energy velocity:

$$\overline{v_{e,eff}} = \overline{v_{e,M}} \cdot \frac{1 - r^2}{1 + r^2}$$

Here $\overline{v_{e,eff}}$ does not describe the forward propagation of the energy or of the photons in an ensemble. In this case the energy transport equals $\overline{v_{e,M}}$, which in turn is the group velocity. This velocity was measured in the tunneling experiments, where the transmitted signal $\overline{P_{trans}}$ and its velocity $\overline{v_{e,M}}$ was detected. In the above presented experiment the velocity of $4.34 \cdot c$ was measured, this in fact is different from the energy transport in a vacuum or any medium M, where $\overline{v_{e,M}} \leq c$ holds.

It should be reminded that the electric field E similar to ψ cannot be measured, only E^2, i.e. the energy, since every detector measures the energy of the photons.

As mentioned above the claimed classical energy velocity as defined in Section 4.1 makes only sense if reflections do not occur. The exponential decay of an evanescent mode or a tunneling probability is due to elastic reflection only.

7.4. *Advanced potentials and evanescent modes*

All the photonic tunneling calculations are based on the causal retarded potentials. The advanced solutions of the Maxwell equations are not considered because they are 'unphysical'. However, they are mathematically equivalent solutions. It should be investigated, whether these solutions describe the propagation of evanescent modes. There are many studies known in which superluminal solutions of the Maxwell equations have been analyzed, see e.g. Recami[74] and quite recently Rodrigues and Lu.[75]

8. SUMMING UP

Analogous tunneling experiments with classical evanescent electromagnetic modes have shown, that in the case of opaque barriers, the signal and the energy velocity can become superluminal. The result are essentially in agreement with the quantum mechanical phase time approach. The mathematical analogy between the one-dimensional tunneling and the propagation of evanescent modes allows the conclusion, that the quantum mechanical phase time is relevant for electronic devices. That means, its intrinsic tunneling time can be calculated.

The question, whether causality may be violated by superluminal signal and energy velocities has not been answered until now. So far the theoretical investigations did not consider the frequency band limitation of the signals and that the front velocity represents a meaningless quantity for solving this problem. As we have discussed in Section 4.2, signals are always frequency band limited and this property allows a superluminal signal velocity in the case of the propagation of evanescent modes.

Acknowledgements—We are very grateful to Dr P. Sen for a critical reading of our manuscript.

REFERENCES

1. I. Giaver, *Phys. Rev. Lett.* **5,** 147 (1960).
2. L. Esaki, *IEEE Trans.* **ED-23,** 644 (1976).
3. G. Binder, H. Rohrer, Ch. Gerber and E. Weibel, *Appl. Phys. Lett.* **40,** 37 (1982).
4. E. H. Hauge and J. A. Støvneng, *Rev. Mod. Phys.* **61,** 917 (1989).
5. V. S. Olkhovsky and E. Recami, *Phys. Rep.* **214,** 339 (1992).
6. R. Landauer and Th. Martin, *Rev. Mod. Phys.* **66,** 217 (1994).
7. R. Landauer, *Nature* **341,** 567 (1989).
8. M. Tsuchiya, T. Matsusue and H. Sakaki, *Phys. Rev. Lett.* **59,** 2356 (1987).
9. A. Enders and G. Nimtz, *J. Phys. I (France)* **2,** 1693 (1992).
10. A. Enders and G. Nimtz, *J. Phys. I (France)* **3,** 1089 (1993).
11. A. M. Steinberg, P. G. Kwiat and R. Y. Chiao, *Phys. Rev. Lett.* **71,** 708 (1993).
12. A. Ranfagni, P. Fabeni, G. P. Pazzi and D. Mugnai, *Phys. Rev. E* **48,** 1453 (1994).
13. Ch. Spielmann, R. Szipöcs, A. Stingl and F. Krausz, *Phys. Rev. Lett.* **73,** 2308 (1994).
14. Th. Hartman, *J. Appl. Phys.* **33,** 3427 (1962).
15. New Scientist, page 26, 1. April 1995; Frankfurter Allgemeine Zeitung, 7. July 1995; Die ZEIT, 21. July 1995; FOCUS, **19,** 214 (1995); BBC London, HORIZON, 2. December 1996.
16. J. Ch. Bose, Bose Institute Transactions, 42 (1927).
17. A. Sommerfeld, Vorlesungen über Theoretische Physik, Band IV OPTIK, Verlag Harri Deutsch Thun, (1989).
18. C. K. Carniglia and L. Mandel, *J. Opt. Soc. Am.* **61,** 1035 (1971).
19. Th. Martin and R. Landauer, *Phys. Rev. A* **45,** 2611 (1992).
20. H. M. Brodowsky, W. Heitmann and G. Nimtz, *Phys. Lett. A* **222,** 125 (1996).
21. A. Ranfagni, D. Mugnai, P. Fabeni and G. P. Pazzi, *Appl. Phys. Lett.* **58,** 774 (1991).
22. G. Nimtz, A. Enders and H. Spieker, *J. Phys. I (France)* **4,** 565 (1994).
23. J. D. Jackson, 'Classical Electrodynamics' 2nd edition. John Wiley, New York, (1975).
24. L. Brillouin, 'Wave Propagation in Periodic Structures' 2nd edition. Dover Publications, Inc., New York, (1953).
25. E. Yablonovitch, *J. Phys. Cond. Matt.* **5,** 2443 (1994).
26. The numerical calculations were carried out by H. Spieker.
27. P. R. Villeneuve and M. Piché, *Prog. Quantum Electronics* **18,** 153 (1994).
28. H. Aichmann and G. Nimtz, to be published.
29. A. Enders and G. Nimtz, *Phys. Rev. E* **48,** 632 (1994).
30. H. Spieker, private communication.
31. A. Enders and G. Nimtz, *Phys. Rev. B* **47,** 9605 (1993).
32. F. Raciti and G. Salesi, *J. Phys. I (France)* **4,** 1783 (1994).
33. D. Mugnai, A. Ranfagni, R. Ruggeri and A. Agresti, *Phys. Rev. E* **49,** 1771 (1994).
34. G. Nimtz, H. Spieker and H. M. Brodowsky, *J. Phys. I (France)* **4,** 1379 (1994).
35. L. Brillouin, Wave propagation and group velocity, Academic Press, New York, (1960).
36. C. G. B. Garrett and D. E. McCumber, *Phys. Rev. A* **1,** 305 (1970).
37. S. Chu and S. Wong, *Phys. Rev. Lett.* **48,** 738 (1982).
38. W. Heitmann and G. Nimtz, *Phys. Lett. A* **196,** 154 (1994).
39. E. Desurvire, *Scientific American*, 96, January (1992).
40. A. Papoulis, The Fourier Integral and its Applications. McGraw-Hill Book Company Inc. New York, (1962).

41. P. Pleshko and I. Palócz, *Phys. Rev., Lett.* **22,** 1201 (1969).
42. W. Heitmann, Bibliography. http://www.uni-koeln.de/Nabb11/lit.ps.92.
43. A. M. Steinberg and R. Y. Chiao, *Phys. Rev. A* **51,** 3525 (1995).
44. R. Landauer and Th. Martin, *Sol. St. Comm.* **84,** 115 (1992).
45. Emig, Th., *Phys. Rev. E,* **54,** 5780 (1996).
46. J. Ruiz, V. Gasparian, M. Ortuño, and E. Cuevas, *J. Phys. I* (France) (1996) (submitted).
47. Heitmann, W. PhD thesis at the University of Cologne, (1997).
48. G. Diener, *Phys. Lett. A,* **223,** 327 (1996).
49. C. R. Leavens and G. C. Aers, in Scanning Tunneling Microscopy III edited by R. Wiesendanger, H.-J. Güntherodt, Springer Series in Surface Sciences, **29,** 105 (1993).
50. P. R. Holland, *Phys. Rep.* **224,** 95 (1993).
51. M. M. Lam and C. Dewdney, *Found. Phys.* **24,** 3 (1994).
52. D. Sokolovski and L. M. Baskin, *Phys. Rev. A* **36,** 4604 (1987).
53. D. Sokolovski and J. N. L. Conner, *Phys. Rev. A* **42,** 6512 (1990).
54. D. Sokolovski and J. N. L. Conner, *Phys. Rev. A* **44,** 1500 (1990).
55. M. Büttiker, *Phys. Rev. B* **27,** 6178 (1983).
56. E. P. Wigner, *Phys. Rev.* **40,** 749 (1932).
57. H. W. Lee and M. O. Scully, *Found. Phys.* **13,** 61 (1983).
58. M. S. Marinov and B. Segev, http://xxx.lanl.gov/ps/quant-ph/9602017.
59. V. F. Rybachenko, *Sov. J. Nucl. Phys.* **5,** 635 (1967).
60. A. I. Baz', *Sov. J. Nucl. Phys.* **4,** 182 (1967).
61. V. Gasparian, M. Ortuño, J. Ruiz and E. Cuevas, *Phys. Rev. Lett.* **75,** 2312 (1995).
62. M. Deutsch and J. E. Golub, *Phys. Rev. A* **53,** 434 (1996).
63. C. R. Leavens and G. C. Aers, *Phys. Rev. B* **40,** 5387 (1989).
64. M. Büttiker and R. Landauer, *Phys. Rev. Lett.* **49,** 1739 (1982).
65. H. M. Krenzlin, J. Budczies and K. W. Kehr, *Phys. Rev. A* **53,** 3749 (1996).
66. Salecker and E. Wigner, *Phys. Rev.* **109,** 571 (1958).
67. C. R. Leavens and W. R. McKinnon, *Phys. Lett. A* **194,** 12 (1994).
68. J. G. Muga, S. Brouard and R. Sala, *Phys. Lett. A* **167,** 24 (1992).
69. S. Brouard, R. Sala and J. G. Muga, *Phys. Rev. A* **49,** 4312 (1994).
70. M. J. Hagman, *Sol. St. Comm.* **82,** 867 (1992).
71. S. M. Sze, 'Physics of Semiconductor Devices' 2nd Edition. John Wiley, New York, (1981).
72. R. Landauer, *Nature* **365,** 692 (1993).
73. H. Aichmann, G. Nimtz, and H. Spieker, Verhandlungen der Deutschen Physikalischen Gesellschaft, 7, 1258, (1995).
74. E. Recami, *Rivista Nuova Cim.* **9,** 1 (1986).
75. W. A. Rodrigues, and J.-Y. Lu, *Found.* **127,** (3) (1997).